Acta Oceanol. Sin., 2024, Vol. 43, No. 9, P. 93–104
https://doi.org/10.1007/s13131-024-2362-3
http://www.aosocean.com
E-mail: ocean2@hyxb.org.cn

Stratification in central Bohai Sea and how it has shaped hypoxic events in summer

Jie Guo[1, 2]*, Diansheng Ji[3], Xiangyang Zheng[1, 2], Yanfang Li[1, 2], Haitian Tang[3], Chawei Hou[3]

[1] CAS Key Laboratory of Coastal Environmental Processes and Ecological Remediation, Yantai Institute of Coastal Zone Research, Chinese Academy of Sciences, Yantai 264003, China

[2] Shandong Key Laboratory of Coastal Environmental Processes, Yantai 264003, China

[3] Yantai Marine Center of the Ministry of Natural Resources, Yantai 264006, China

Received 24 April 2024; accepted 4 June 2024

Abstract

In the last 10 years (2012–2021), five hypoxic events have been observed in summer in the central Bohai Sea (CBS). Frequent and persistent hypoxia will have an impact on the ecosystem of the CBS. In this paper, historical sea temperature (ST), salinity (SAL), density (Den), and dissolved oxygen (DO) concentration data from three stations in the CBS are analyzed via the linear regression method, and the correlations between the stratification factors (ST, SAL, and Den) and DO concentration are determined. The thresholds of the stratification factors at the three stations in June in the year in which hypoxia occurred were determined and applied to survey data from 29 stations in late May to early June in 2022 in the CBS; this assessment found that the data from 19 stations indicated that hypoxia was about to occur. In August, the survey data showed that 14 out of the 29 stations indicated hypoxic conditions, of which 12 were from the predicted 19 stations, meaning that the estimation accuracy reached 63%. The same approach was applied to data from June 2023. The data for August from a bottom-type online monitoring system in the CBS verified the occurrence of hypoxic events around Sta. M2. The results show that the strength of the seawater stratification plays a leading role in hypoxic events in the summer in the CBS, and the thresholds of the stratification factors can be used to predict the occurrence of hypoxic events.

Key words: hypoxia, central Bohai Sea, sea temperature, salinity, sea-water density, stratification

Citation: Guo Jie, Ji Diansheng, Zheng Xiangyang, Li Yanfang, Tang Haitian, Hou Chawei. 2024. Stratification in central Bohai Sea and how it has shaped hypoxic events in summer. Acta Oceanologica Sinica, 43(9): 93–104, doi: 10.1007/s13131-024-2362-3

1 Introduction

The dissolved oxygen (DO) in seawater is key to shaping the growth and reproduction of marine organisms. It is an important contributor to the biogeochemical cycle. Overall, the magnitude of the DO concentration reflects the health of an aquatic system. Hypoxia occurs when the rate of oxygen consumption in seawater exceeds the rate at which it is replaced. When the DO concentration in seawater is as low as 3–4 mg/L, many marine organisms are adversely affected (Diaz, 2001; Wu, 2002; Vaquer-Sunyer and Duarte, 2008; Zhai et al., 2012). At DO concentration values of less than 3 mg/L, certain fish begin to die, and the number of benthic organisms is greatly reduced. When the DO is completely consumed, i.e., oxygen-free (no oxygen), which results in anoxia, most marine life cannot survive (Li et al., 2002; Zhang et al., 2010; Zhai et al., 2012). Therefore, selecting different hypoxia thresholds in different regions is beneficial to accurately assessing the occurrence of hypoxic events.

Biochemical processes involving oxygen consumption and water stratification (e.g., density differences) hinder the exchange between water surface with high levels of oxygen and hypoxic bottom water, which directly causes hypoxia (Turner et al., 1987; Rabalais et al., 2002; Hetland and Dimarco, 2008). Taft et al. (1980) pointed out that fresh water increased density stratification in Chesapeake Bay in spring, resulting in hypoxia of the water below a depth of 10 m. In addition, studies have also shown that hypoxic areas such as Chesapeake Bay (Hagy et al., 2004) and the middle of the Baltic Sea (Conley et al., 2002) are related to the submarine topography. Rabalais et al. (2007, 2010) found that the Mississippi River Estuary injected a large amount of fresh water and excess nutrient salts into the northern part of the Gulf of Mexico. This large amount of hot fresh water promoted the formation of high-density stratified structures in summer, and the input of excess nutrient salts led to intensification of the water eutrophication. The combination of these two processes induced the formation of seasonal hypoxia at the bottom. The hypoxia at the bottom of the Changjiang River Estuary in summer is caused by the large quantity of nutrients carried by diluted water, leading to stratification and a marked increases in primary productivity (Li et al., 2002; Luo et al., 2005; Zhang et al., 2007; Wei et al., 2007; Chen et al., 2007). The degree of summer hypoxia is correlated with the magnitude of the river flux in estuary/inshore areas that are controlled by runoff water. Increased nutrient delivery can increase the primary productivity and lead to oxygen consumption, but it can also decrease the residence time and increase flushing, reducing the duration of hypoxic events, such as those in the Chesapeake Bay, Neuse, and Pamlico estuaries in the United States and in the Black Sea, Adriatic Sea, German Gulf, and North Sea in Europe (Diaz, 2001; Lin et al., 2006, 2008; Hagy et al., 2004).

The Bohai Sea (BS) is a semi-enclosed sea connected to the

Foundation item: The National Natural Science Foundation of China under contract Nos U2106211 and 42076197.
*Corresponding author, E-mail: jguo@yic.ac.cn

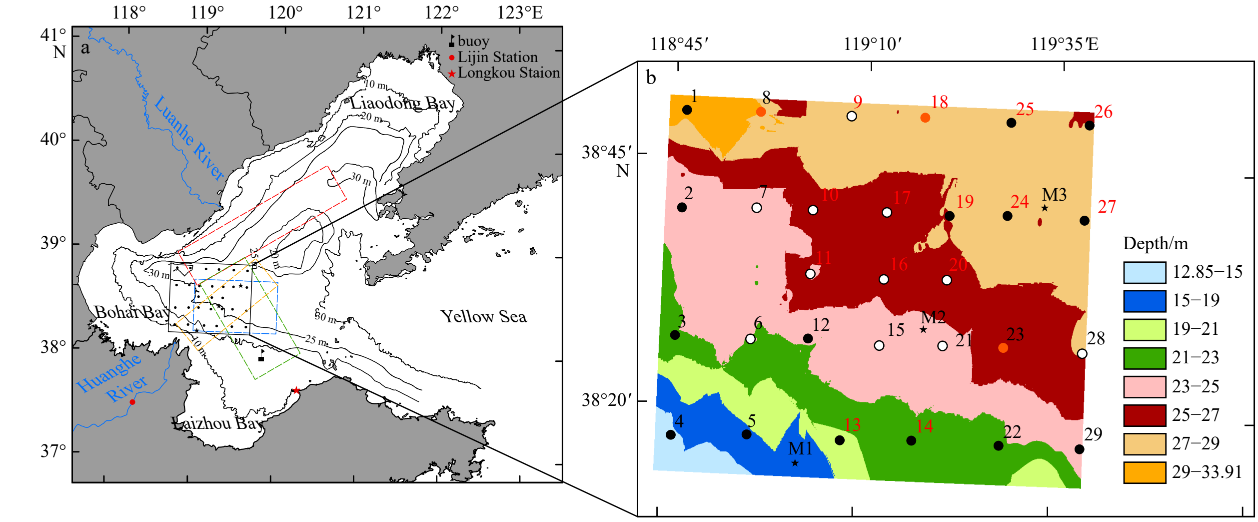

Fig. 1. Locations of survey stations in the CBS (Stas M1, M2, and M3). a. The black box is the study area; b. twenty-nine stations were distributed in the study area. In a, the yellow, blue, red, and green dashed boxes denote the hypoxic zones investigated by Zhang et al. (2016), Jiang et al. (2016), Zhai et al. (2012), and Li et al. (2021), respectively. The black contours and values indicate the water depth (in unit of m). In b, the black dots indicate DO concentration values of ⩾4 mg/L, the white dots indicate DO concentration values of 3–4 mg/L, and the red dots indicate DO concentration values of <3 mg/L in summer in 2022; the black numbers indicate before strong winds, and the red numbers indicate after strong winds during the summer in 2022.

Yellow Sea through an opening east of the Bohai Strait (Fig. 1). It is very shallow and has a mean depth of 18 m. The general circulation pattern of the BS is shaped by seawater, which enters north of the Bohai Strait and exits in the south. This trend results in the entire BS having an anticlockwise circulation (Huang et al., 1999; Wang et al., 2010; Ding et al., 2019; Wu et al., 2019). Many rivers, such as the Huanghe and Haihe rivers, converge in the BS area. These rivers carry large amounts of organic materia from the inland region, making the BS a natural fishing ground that is rich in seafood such as shrimp, crab, and yellow croaker. The spawning and breeding periods of economically important fish, shrimp, and crab in the BS are between March and August. The deep-water area in the central BS (CBS) is the distribution center for the migration of organisms of dietary importance. However, it acts as their wintering ground. With the rapid economic development and urbanization of the Bohai Rim region, the flux of land-based pollutants into the sea has increased. According to the 2015 Marine Environment Bulletin of the Beihai Region, from 2001 to 2015, the coastal waters of the BS became increasingly polluted, and this pollution manifested as the frequent occurrence of red tides. The waters that underwent eutrophication were mainly located in the top of Liaodong Bay, Bohai Bay, and Laizhou Bay. Shellfish tend to be plagued by frequent red tides due to increased eutrophication in these three major bays of the BS (Bulletin of the State of the Marine Environment of China, 2010). For example, in the summer of 1997 and 1998, many farmed scallops died in the coastal waters around the BS (Zhai et al., 2012), most likely due to hypoxia. Hypoxic events in the CBS often occur near double-centered cold water masses (DCCWM). Wei et al. (2021) analyzed data for August acquired from a station near the cold water mass near the northern BS using the National Oceanic Standard Profile Measurement dataset (1978–2018). They reported that severe oxygen depletion occurred during the summer from 2006 to 2018. Zhai et al. (2012) investigated DO concentration and pH data from 20–23 stations in and around the CBS for June and August 2011. They found that the DO concentration of the bottom water decreased significantly and that the water was acidified in a zonal area at depths of 20–35 m in the northwest and northern coastal regions of the BS (red dashed boxes in Fig. 1a). Zhang et al. (2016) conducted a summer survey of the BS in 2014. They reported that the formation of a seasonal thermocline in summer was the main physical process in the hypoxic zone at the bottom, and the oxygen consumption of mineralization and decomposition processes was also the reason for the formation of a hypoxic zone. The total area in the CBS with DO concentration values of <3 mg/L was approximately 4.2×10^3 km^2 (yellow dashed boxes in Fig. 1a). In the summer of the same year, Jiang et al. (2016) reported DO concentration values of <3 mg/L in the cold water mass near the southeastern BS, and the lowest value reached 2.3 mg/L (blue dashed boxes in Fig. 1a). They suggested that the long-term water stratification and the existence of more organic matter in the water has laid the foundation for the formation of the hypoxic zone. Using observational data obtained during the summer of 2019. Li et al. (2021) found that the area of hypoxia extended from the depression on the west side of the shoal in 2014 to the area around the mouths of the Huanghe River and the Laizhou Bay (green dashed boxes in Fig. 1a). The frequent occurrence and expansion of hypoxic events will directly affect the ecological environment in the CBS.

The hypoxic events in the CBS mentioned above all occurred in the area of the DCCWM. Zu et al. (2005) reported that the DCCWM was characterized by low temperatures and high salinity, and the DO concentration was lower than that in the surrounding area (Wei et al., 2019). Bao et al. (2004) suggested that the formation of DCCWM low-temperature zones may be closely related to the existence of a topographic trough in the BS and may result from the extension of the east and west low-temperature centers along this deep trough. Zhou et al. (2017) discovered the presence of a basin-scale cyclonic gyre induced by the DCCWM in summer in the BS, and the circulation potentially contributed to the development of hypoxia in this region.

The stratification of seawater is the hierarchical structure of the sea temperature (ST), salinity (SAL), and density (Den) of seawater with depth. Huang et al. (1999) suggested that seawater stratification is one of the causes of hypoxia in the BS. Stratification occurred in the BS from April to August, during which it gradually strengthened as the temperature increased and ended around mid-September (Huang et al., 1999; Zhou et al., 2017).

Based on discontinuous historical observational data from three stations in the CBS from 2013 to 2022, we studied the correlation between the stratification factor and the DO concentration via the linear regression method and analyzed the formation process of stratification during different months to determine the time at which the occurrence of hypoxia should be evaluated and verified. The results of this study enhance the understanding of the effect of stratification on hypoxia in the CBS and provide further references for early warning of hypoxia in the CBS.

2 Data and methods

2.1 *Historical data*

The historical data were obtained from the Yantai Institute of Coastal Zone Research, Chinese Academy of Sciences (CAS), China, and were collected from Stas M1, M2, and M3 in the CBS (Fig. 1), which represent different water depths in the study area. The data included ST, SAL, Den, and DO concentration data, which were collected during a non-continuous comprehensive survey of the BS from 2013 to 2022. Observational data from the conductivity, temperature, and depth (CTD), SBE19+ CTD, and SBE25+ CTD (Sea-Bird Electronics, Inc., Bellevue, WA, USA) were used to determine the ST, SAL, and Den *in situ*. The DO concentration was measured using an SBE43 sensor. The field survey data were subjected to quality control and processing before being used in the subsequent analysis. The first step was to discard the ST, SAL, Den, and DO concentration data for outside the range boundaries provided in the user manual of the World Ocean Database 2018 [see Locarnini et al. (2018) Appendix 11 for min-max values of temperature, salinity, and DO concentration in coastal areas of the North Pacific]. The quality-controlled data were then interpolated to standard levels at 1 m vertical intervals. The air temperature (T) data were obtained from the Longkou Meteorological Station, and the Huanghe River runoff into the sea were obtained from the Lijin Hydrological Station. Sea surface temperature (SST) data from a buoy in the CBS were processed and analyzed by the Yantai Marine Center of the Ministry of Natural Resources, China.

2.2 *Real-time survey data*

The study area is located in the cold water mass in the southern BS (black rectangle in Fig. 1a). Real-time sea survey data (i.e., ST, SAL, Den, and DO concentration data) from May 28 to June 2 (June for short) and August 30 to September 4 (August for short), 2022, including data for the upper (0.5 m), middle (10 m), and bottom (2 m from the sea floor) three layers, from 29 stations, ranging from dense (Stas 10, 17, 19, 11, 16, 20, 12, 15, and 21) to scattered, were obtained. Stations intervals of 7.5 nautical miles horizontally and 6.5 nautical miles longitudinally in the dense area were established (Fig. 1b). The average distance between the other stations was approximately 10 nautical miles. The data were obtained using a YSI ProPlus multiparameter water quality analyzer (YSI, Inc., Yellow Springs, OH, USA) from late May through early June, as well as in August, in 2022. The SAL measurements were calibrated against standard seawater. The DO settings were calibrated using the water-saturated air method prior to each voyage.

2.3 *Data from a base-type online monitoring system*

A base-type online monitoring system (BTOMS) was deployed at Sta. M2 (Fig. 1b) on the seabed in the CBS from June to August in 2023. The data were acquired (Table 1) at an interval of 1 h. The BTOMS was equipped with a YSI EXO2 multiparameter water quality analyzer, which contained a depth sensor (strain gauge pressure principle), DO sensor (fluorescence method), total algae sensor (fluorescence method), conductivity/temperature composite sensor (thermistor principle), and pH sensor (glass composite electrode method).

2.4 *Stratification factors and DO characteristic analysis methods*

The regression analysis method (RAM) was used to analyze the historical data. Taking data from Sta. M2 as an example, the characteristics of the stratification factors (ST, SAL, and Den) and DO concentration over time were analyzed. The month of the initial formation of the stratification was also determined. A general global optimization algorithm was used to simulate the correlations between the DO concentration and the ST, SAL, and Den with depth and to simulate the correlations between the DO concentration and the ST, SAL, and Den values of the upper layer minus the values of the bottom layer (Δ) from 2013 to 2022. The roles of the stratification factors in the hypoxic events was also determined. The thresholds of the stratification factors during the month in the early formation stage of the stratification during hypoxic events were determined. The method of determining the thresholds of the stratification factors for Stas M1 and M3 was the same as that for Sta. M2. The thresholds of the stratification factors at these three stations were applied to the survey data for 2022 and 2023 to estimate the likelihood of the occurrence of hypoxia at each station. The workflow of our research is shown in Fig. 2c.

2.5 *Observation depths of the 29 stations matched with Stas M1, M2, and M3*

As shown in Fig. 2a, there was a correlation between the DO concentration values at the bottom of the study area and the depth at the same station in spring in 2022. The different depths of the historical data for Stas M1, M2, and M3 were collected in the study area and the sites gradually deepened from southwest to northeast (Fig. 1b). Because the depth of the observations was usually approximately 2 m from the seabed, in order to better compare the analysis data with the historical data, we matched the observed depths of the 29 stations with the observed depths close to Stsa M1, M2, and M3 (Fig. 2b).

Table 1. Data sources of historical and real-time

Data classification	Time	Station	Data
Historical data	2013–2022	M1, M2, M3	ST, SAL, Den, DO concentration
	2011–2022	Longkou Station	T
	2010–2022	Lijin Station	Huanghe River runoff
Real-time data	June and August in 2022	Stas 1–29	ST, SAL, Den, DO concentration
	June–August in 2023	M2	ST, SAL, Den, DO concentration
	June–August in 2023	buoy	SST, SAL

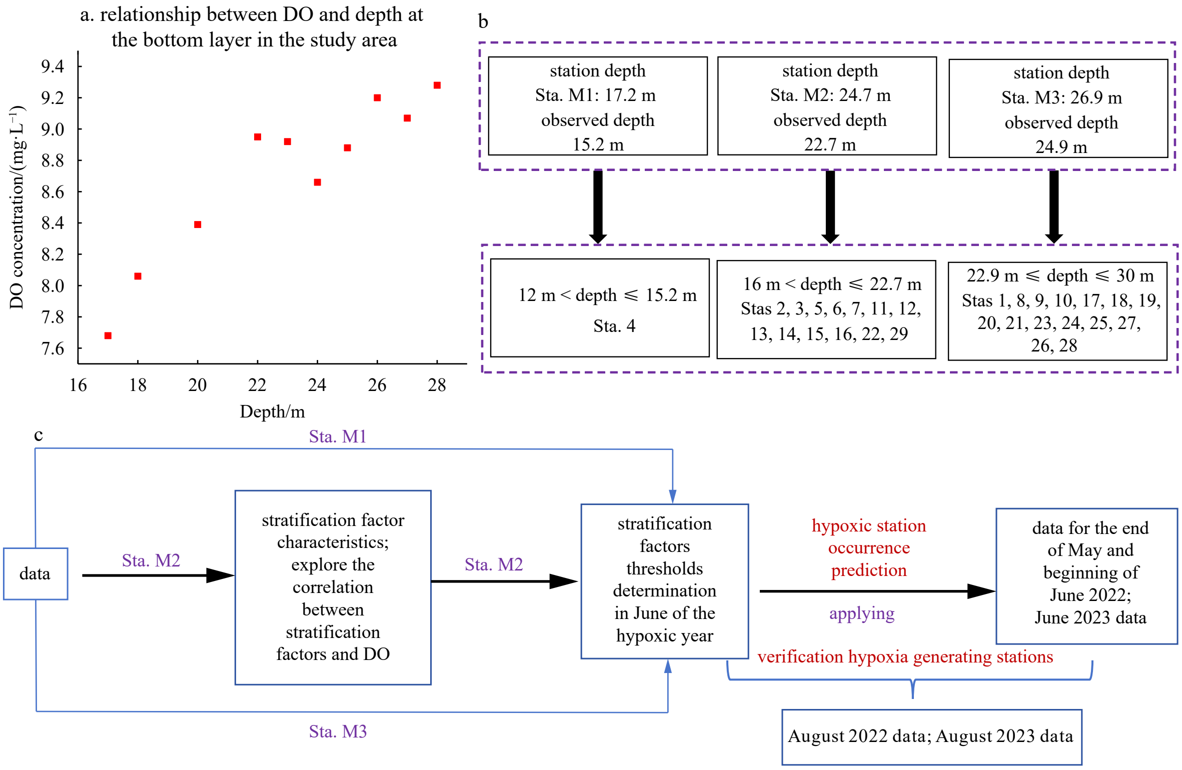

Fig. 2. Research methods: a. the correlation between the bottom DO concentration and water depth in the study area in spring 2022; b. the observation depth range for the 29 stations (Stas 1–29) in the study area corresponds to that of Stas M1, M2, and M3; and c. the workflow of our research.

2.6 *Hypoxic environment threshold settings in the study area*

The seawater quality was divided into Class 1 (DO concentration > 6 mg/L), Class 2 (DO concentration > 5 mg/L), Class 3 (DO concentration > 4 mg/L), and Class 4 (DO concentration > 3 mg/L). Classes 1 and 2 were good water bodies, that is, healthy water bodies. In contrast, water bodies with DO concentration values of <4 mg/L were unhealthy water bodies (National Standard of the People's Republic of China: Standard for Seawater Quality, UCD 551463 GB3097-1997). In this study, environments with DO concentration value of <4 mg/L were defined as a hypoxic environments in order to predicate hypoxic events.

Some datasets for this research are included in this paper and will be made available upon request at https://www.scidb.cn/.

3 Results

3.1 *Distribution characteristics of stratification factors and DO concentration at Sta. M2 in the CBS*

The data were derived from the accumulated voyage survey data at Sta. M2 from 2013 to 2022 (discontinuous, no fixed survey period) (Fig. 3). To achieve a better comparison, the data for December, February (dotted line), and April–June (*line) are plotted in Figs 3a, c, e, and g, and the data for August (line) and November (○line) are plotted in Figs 3b, d, f, and h. Figures 3a and b show that the ST from the upper and bottom layers in the CBS were basically uniform in December and February. The ST stratification began in April, and an obvious thermocline formed in June. In August, the thermocline strengthened further and the water depth was 5–10 m, the maximum ST difference in the thermocline was 5.5℃, and the ST outside the thermocline only changed slightly. The stratification gradually disappeared after August.

The SAL distribution is shown in Figs 3c and d. In December and February, the SAL of the subsurface layer increased, after which the SAL changed little with depth; SAL stratification initially appeared in April. The SAL was strongly stratified due to external influences in April 2022. The variation trend of halocline in June, August, and after August were the same as that of the thermocline. The halocline was mainly stable in water depths of 5–10 m, the maximum SAL difference was 0.6, and the SAL only changed slightly in the regions outside the halocline.

Both the thermocline and halocline gradually strengthened with increasing sea surface temperature. Because the density of sea water is related to the SST and salinity, the pycnocline, thermocline, and halocline had the same change trends in April, June, August, and after August. The pycnocline formed at a depth of 5–10 m (Figs 3e and f).

Figures 3g and h show that the change in the loss of DO concentration with depth was not obvious in December, February, April, and May. It began to become obvious in June, and the trend of the loss of DO concentration further increased in August. At depths of 5–10 m, the DO concentration value exhibited a decreasing trend; and at depths of 10–15 m, the DO concentration value exhibited a larger decreasing trend, that is, beneath the stratification of seawater (at a depth of 5–10 m below), the DO concentration value exhibited a large trend of depletion at depths of 10–15 m.

It was found that seawater stratification initially formed in June, and the oxygen consumption at the bottom initially appeared in June. In August, the stratification was enhanced and the oxygen consumption in the bottom layer was enhanced.

3.2 *Correlation analysis between DO concentration and ST, SAL, and Den at Sta. M2 in the CBS*

A total of 79 sets of data were obtained for February, June, August, and December in 2017. The simulation results were evalu-

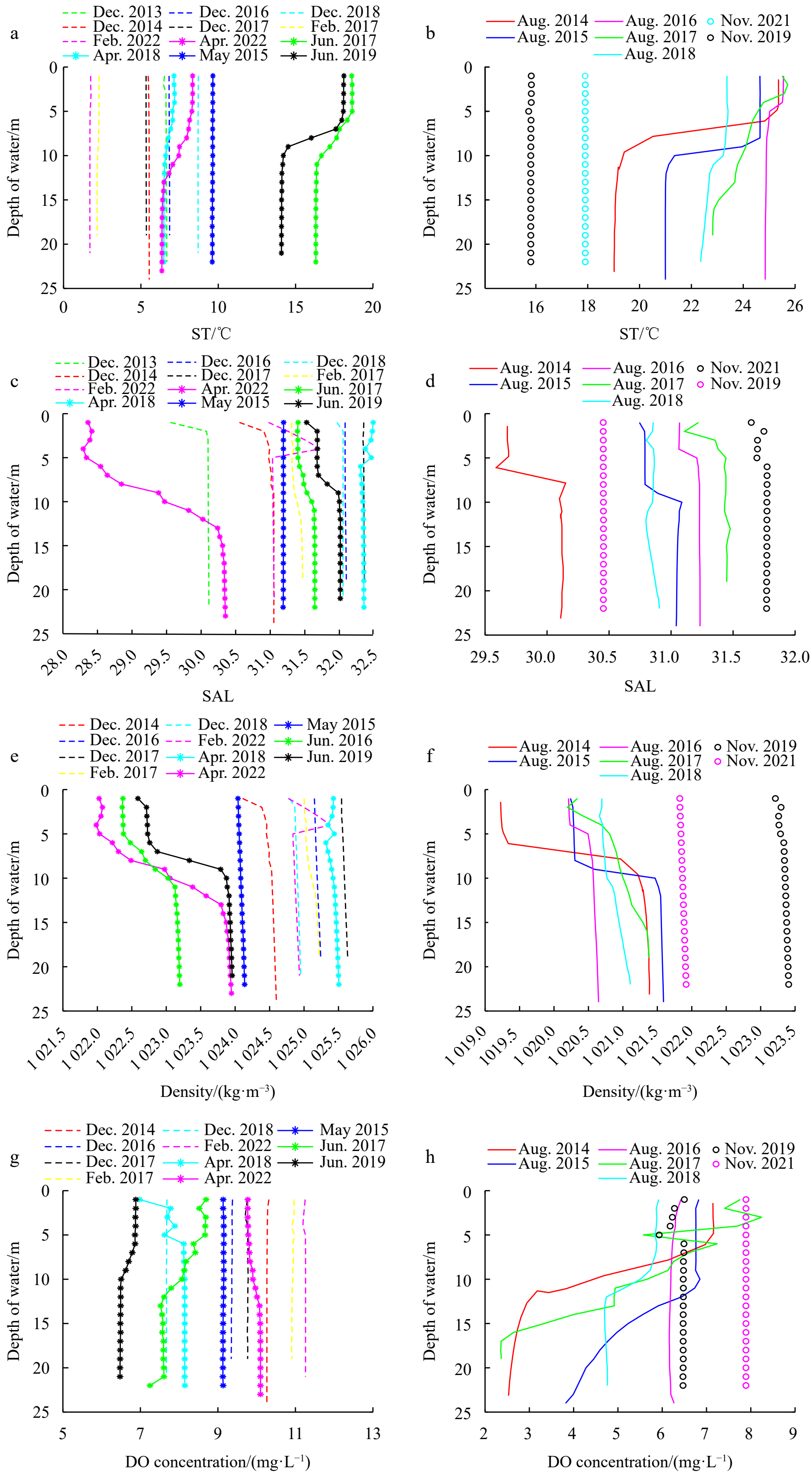

Fig. 3. Variations in the ST, SAL, Den, and DO concentration with depth in different seasons at Sta. M2 in the CBS from 2013 to 2022. a. ST from winter and spring, b. ST from summer and autumn, c. SAL from winter and spring, d. SAL from summer and autumn, e. density from winter and spring, f. density from summer and autumn, g. DO concentration from winter and spring, and h. DO concentration from summer and autumn. To achieve a better comparison, the data for December, February (dotted line), and April–June (*line) are plotted in Figs 3a, c, e, and g, and the data for August (line) and November (○line) are plotted in Figs 3b, d, f, and h.

ated using the correlation coefficient (R), root mean square error (RMSE), residual sum of squares (SSE), R-squared, and the determination coefficient (DC) using a general global optimization algorithm.

The correlations between the simulated stratification factors and DO concentration with seawater depth (depths of 1–25 m, n = 79) are shown in Table 2. The correlation coefficients of the ST, SAL, and Den with DO concentration are 0.91, 0.45, and 0.81, respectively. The RMSE values are 0.97 mg/L, 2.06 mg/L, and 1.34 mg/L, respectively. The R-squared values are 0.84, 0.20, and 0.66, respectively. The simulation of the correlation between the ST and DO concentration are the best, followed by the results of the correlation between the DO concentration and the Den, and the results for the correlation between the DO concentration and the SAL are the worst.

The simulated correlations between the ΔDO and the ΔST, ΔSAL, and ΔDen are shown in Table 2. The R values of the correlations between the ΔDO and the ΔST, ΔSAL, and ΔDen are 0.82, 0.78, and 0.81, respectively, which are close to each other. The RMSE values are 0.96 mg/L, 1.05 mg/L, and 0.97 mg/L, respectively, and the R-Squares values are 0.66, 0.61, and 0.67, which are relatively close.

Based on a comparison of the simulation results, it is reasonable to use the ΔST, ΔSAL, and ΔDen values to evaluate the occurrence of hypoxia. Stratification plays a leading role in the occurrence of hypoxia at Sta. M2.

3.3 *Thresholds of stratification factors at Sta. M2*

In the CBS, stratification occurred in June and was further strengthened in August, in which the largest DO concentration loss occurred. In this section we determine the stratification factor thresholds in June during hypoxia years, and we pre-analyze the possibility of hypoxic events occurring in August.

We analyzed historical data and published articles for the years in which hypoxia occurred in summer (2014, 2015, 2017, 2019, and 2020) in the CBS. As can be seen from Fig. 3h, the minimum DO concentration value (2.37 mg/L) of the bottom layer in the CBS occurred in August 2017.

Due to the discontinuous nature of the observational data, we only had stratification factor data for hypoxic events in June in 2017 and 2019 (Fig. 3). In June 2017, the values of the stratification factors (ΔST, ΔSAL, ΔDen, and ΔDO) were 2.32℃, −0.24, −0.83 kg/m^3, and 1.45 mg/L, respectively. In June 2019, the values of these stratification factors were 4.04℃, −0.49, −1.37 kg/m^3, and 0.41 mg/L, respectively. The absolute values of the stratification factors were all higher in 2019 than in 2017, but the ΔDO value was much smaller in 2019 than in 2017. Figure 4a shows the observed Huanghe River runoff in spring and summer at Lijin Station in the Huanghe River Estuary from 2010 to 2023. In both the spring and summer in 2017, the Huanghe River runoff (HRRF) was lower than the multi-year seasonal average, indicating that the hypoxia in summer in 2017 was less affected by the HRRF into the sea. Figure 4b shows the difference between the air temperature T at Longkou Station and the SST at the buoy in the CBS during spring and summer from 2011 to 2023. The difference between T and SST in the spring and summer in 2017 was lower than the multi-year seasonal average and was the smallest, indicating that T and SST in 2017 were less affected by the unusual weather. The values in 2019 were greater than the multi-year average. Therefore, we selected the stratification factors in June 2017 as thresholds (ΔST ⩾ 2.32℃, ΔSAL ⩽ −0.24, and ΔDen ⩽ −0.83 kg/m^3) to assess that the hypoxia in August in the CBS was reasonable.

3.4 *Characteristics and thresholds of the stratification factors at Stas M1 and M3*

In Figs 5a and b, the red line represents the ST value at Sta. M1. As the water depth at Sta. M1 (17.2 m) is shallow, the ST stratification was not obvious in June or August. The thermocline at Sta. M3 initially formed in June and was further strengthened in August. The thermocline was mainly llocated at depths of 10–15 m. Figures 5c and e show that the SAL and Den at Sta. M1 were stratified in June, and the depths of the stratifications were all 0–5 m. The SAL stratification disappeared in August (Fig. 5d), and the Den stratification did not strengthen (Fig. 5f). As a result, in August, the DO concentration (Fig. 5g) at Sta. M1 did not reach hypoxic conditions (DO concentration < 4 mg/L). The development of the halocline (Figs 5c and d) and density cline (Figs 5e and f) at

Table 2. Simulation results of the correlations between the stratification factors and DO concentration

Correlation	ST/℃ and DO concentration/(mg·L^{-1})	SAL and DO concentration/(mg·L^{-1})	Density/(kg·m^{-3}) and DO concentration/(mg·L^{-1})
y	DO concentration	DO concentration	DO concentration
x	ST	SAL	Density
Formula	$Y = 10.482 - 0.002x^{2.5} + 4.42 \times \exp(x)$	$Y = 10.08 - 3.6/\{1 + [(x - 31.54)/0.14]^2\}$	$y = 5.7 \times 10^6 - 1.67 \times 10^4 x + 16.27 \times x^2 - 5.3 \times 10^{-3} x^3$
R	0.91	0.45	0.81
RMSE/(mg·L^{-1})	0.97	2.06	1.34
SSE	74.62	335.06	141.52
R-squared	0.84	0.20	0.66
DC	0.82	0.20	0.66
Correlation	ΔST/℃ and ΔDO concentration/(mg·L^{-1})	ΔSAL and ΔDO concentration/(mg·L^{-1})	ΔDen/(kg·m^{-3}) and ΔDO concentration/(mg·L^{-1})
y	ΔDO concentration	ΔDO concentration	ΔDO concentration
x	ΔST	ΔSAL	ΔDen
Formula	$y = 3.36 \times \exp[-\exp(110.06 - 47.53x)]$	$y = \exp[-25.74 + 82.61x^3 + 21.82\exp(-x)]$	$y = (0.69 + x)/(8.04 + 7.84x) - 1.05x$
R	0.82	0.78	0.81
RMSE/(mg·L^{-1})	0.96	1.05	0.97
SSE	17.64	20.77	17.99
R-squared	0.66	0.61	0.67
DC	0.66	0.60	0.66

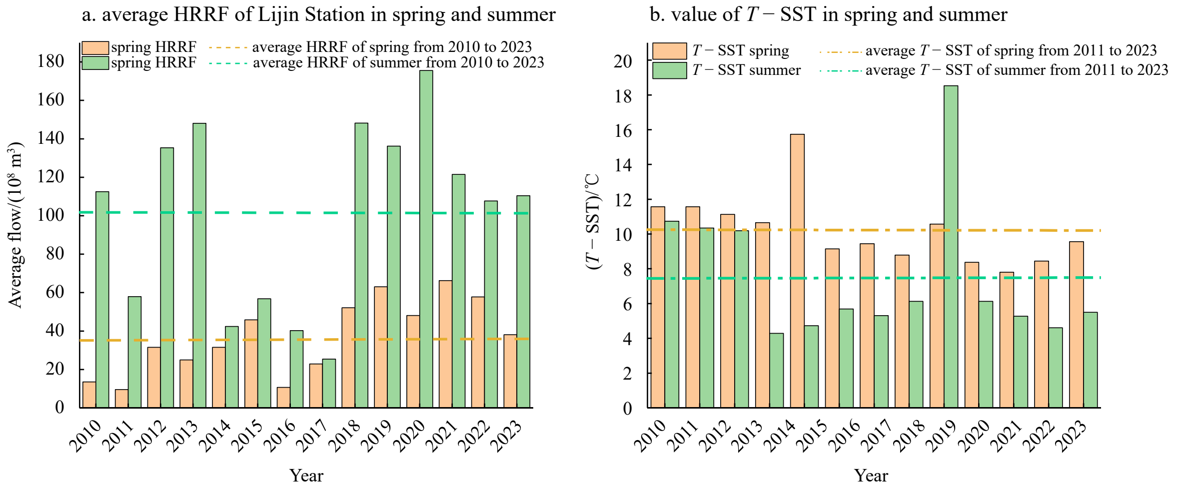

Fig. 4. HRRF at Lijin Station and the air temperature T at Longkou Station minus the SST at the buoy statistics: a. the HRRF of spring and summer at the Lijin Station from 2010 to 2023, and b. the difference between T at Longkou Station and the SST at the buoy in the CBS in spring and summer from 2011 to 2022.

Sta. M3 in June and August was consistent with that of the thermocline. As can be seen from Fig. 5g, at Sta. M3, the DO concentration decreased at depths of 10–15 m in the stratified interval, and it decreased faster below the stratified interval. Comparison of the data for Stas M2 and M3 revealed that they were both located in areas with low flow velocities (Fig. 5h). The current velocity around Sta. M1 was between 0.7 m/s and 0.9 m/s (Zheng et al., 2021). The depth was 2.2 m deeper at Sta. M3 than at Sta. M2, resulting in the depth of the stratification layer at Sta. M3 being lower than that at Sta. M2. The determination of the stratification factor threshold for Sta. M3 in June was also based on the data for 2017, and the method of determining the threshold value was the same as that for Sta. M2. The stratification factor thresholds (SFTs) for the three stations at different depths in the study area are shown in Table 3.

3.5 *Application of SFTs*

A survey was conducted in the CBS from June, 2022, at 29 stations in the upper, middle, and lower layers (Fig. 1b). ST, SAL, Den, and DO concentration data for 29 stations were obtained. The SFTs in June (Table 3) were applied to the stratification factors at 29 stations in June 2022. According to the results presented in Fig. 2b, the observation depths at the 29 stations were matched with the data for Stas M1, M2, and M3, and the SFTs determined using these three stations in June were used to predict whether hypoxia occurred in August at the 29 stations. The evaluation results are shown in Table 4. Only Sta. 4 corresponded to the depth at Sta. M1, and the possibility of hypoxia occurring was very small and thus is not listed on the Table 4. Thirteen stations were judged based on the Sta. M2 SFTs, and seven stations (Stas 7, 11, 12, 14, 15, 16, and 22) reached these SFTs in June. Meanwhile, 15 stations were evaluated based on the Sta. M3 SFTs, and 12 stations (Stas 9, 10, 17, 18, 19, 20, 21, 23, 24, 25, 27, and 28) reached these SFTs in June. That is, according to the stratification factor assessment in June 2022, 19 stations would experience hypoxia in August.

A summer survey was conducted from August 30 to September 4, 2022, in the CBS. However, between August 31 and September 2, gale force winds of 6 (Beaufort scale: wind speed between 10.8 m/s and 13.8 m/s) and above occurred, and the ship was sheltered in the port. The DO concentration and ▲DO values (the bottom layer DO concentration in spring minus the bottom layer DO concentration in summer) of the bottom layer at the 29 stations are shown in Fig. 6. A total of 14 stations (Stas 6, 7, 8, 9, 10, 11, 15, 16, 17, 18, 20, 21, 23, and 28) had DO values of <4 mg/L of which three stations (Stas 8, 18, and 23) had DO concentration values of <3 mg/L, and the minimum DO concentration value occurred at Sta. 8 (DO = 2.92 mg/L) (Fig. 6a). Twelve stations confirmed that the June assessment had an accuracy of 63%. As can be seen from Fig. 6b, the ▲DO values at the hypoxic stations were basically greater than 4 mg/L (except for Sta. 28, ▲DO = 3.92 mg/L). The hypoxic zone was boot-shaped.

A BTOMS was deployed on the seabed at Sta. M2 (Fig. 1b) in the CBS from June to August 2023. Although the ST, SAL, and Den of sea surface were not measured by the BTOMS at Sta. M2, the observed values at the buoy near the study area are representative to a certain extent. Figure 6c shows the stratification factors (ΔST, ΔSAL, and ΔDen) of the sea surface values observed by the buoy minus the seafloor values observed by the BTOMS in June 2023. The dotted line represents the SFTs at Sta. M2 in June (Fig. 6c). The stratification factors from the buoy and BTOMS fully satisfy the SFTs. It was predicted that a hypoxic event would occur at Sta. M2 in August. Figure 6d shows the valid DO concentration data for August 1–20, 2023, some of the DO concentration values were <4 mg/L from August 2 to 12. The DO concentration gradually decreased from August 12 to 20, and all of the values were lower than 4 mg/L. Hypoxic events occurred at Sta. M2 in August 2023.

4 Discussion

4.1 *Validity and rationality of the historical data for the CBS*

Despite the discontinuous nature of the observed data in the CBS and the limited range of the data, it was determined that the stratification in the CBS basically formed in June, and the intensification in August was the best time to observe the hypoxia. Stratification occurred in the CBS from April to August. During this time, it gradually strengthened as the temperature increased. This is consistent with the results of Huang et al. (1999) and Zhou et al. (2017).

The correlation analysis of the stratification factors and DO concentration with depth revealed that the correlation coeffi-

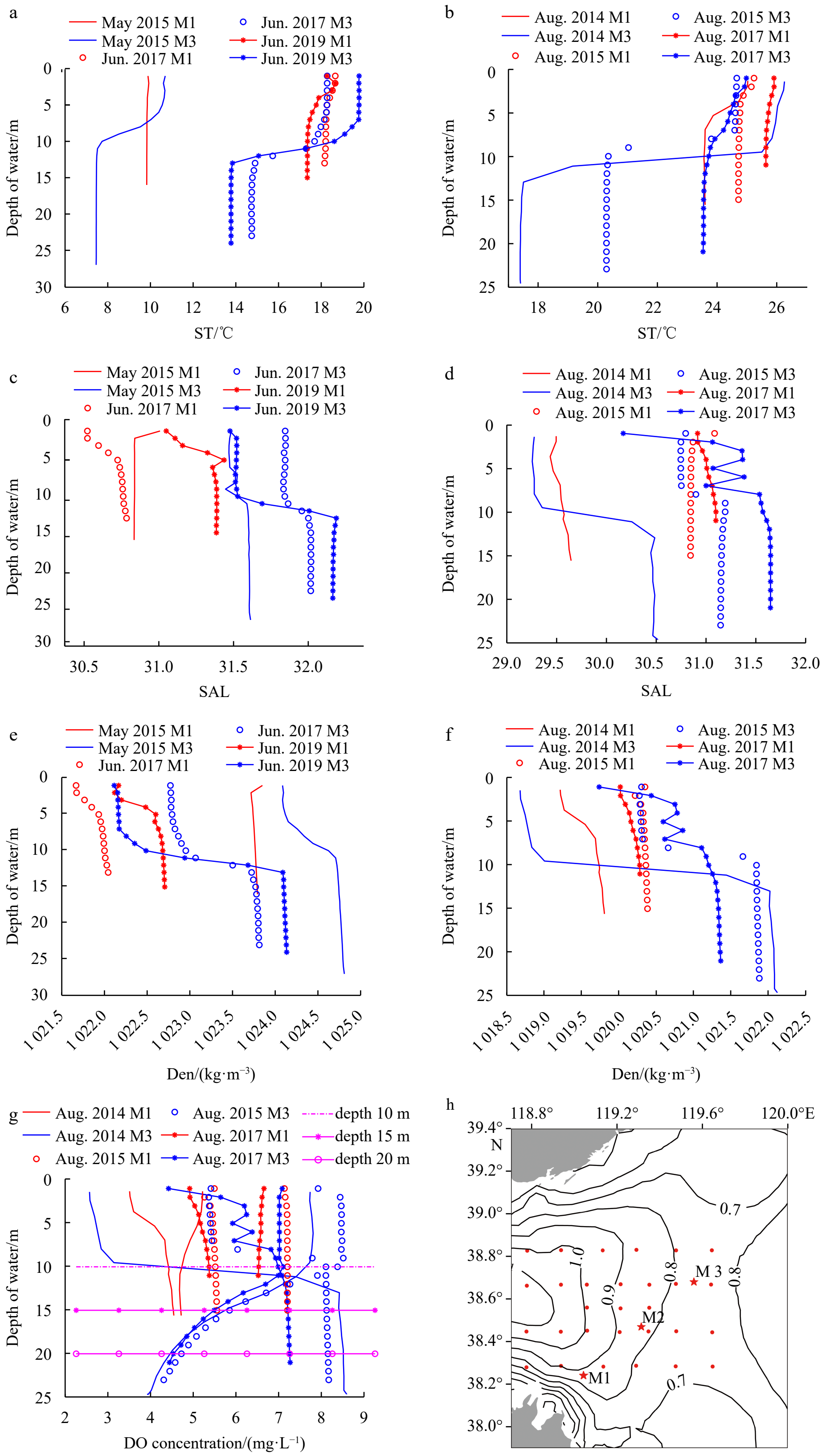

Fig. 5. Information about the stratification factors and DO concentration at Stas M1 and M3 and distribution of flow field in the CBS. a. ST distribution with depth in May and June in 2015, 2017, and 2019; b. ST distribution with depth in August in 2014, 2015, and 2017; c. SAL distribution with depth in May and June in 2015, 2017, and 2019; d. SAL distribution with depth in August in 2014, 2015, and 2017; e. Den distribution with depth in May and June in 2015, 2017, and 2019; f. Den distribution with depth in August in 2014, 2015, and 2017; g. DO concentration distribution with depth in August in 2014, 2015, and 2017; and h. the maximum tidal current velocity in May 2022. In h, red dots: stations; red star: Stas M1, M2 and M3; contour lines and numbers represent the velocity (m/s) of the flow.

Table 3. SFTs for Stas M1, M2, and M3 in June during a hypoxia year

Item	Value		
	Sta. M1	Sta. M2	Sta. M3
ΔST/°C (assessment SFTs of hypoxia in June)	–	⩾2.32	⩾3.54
ΔSAL (assessment SFTs of hypoxia in June)	–	⩽−0.24	⩽−0.17
ΔDen/(kg·m^{-3}) (assessment SFTs of hypoxia in June)	–	⩽−0.83	⩽−1.04

Note: – indicates that there is no threshold.

Table 4. Assessment of the stratification factors for June, 2022

Station	Sta. M2			Station	Sta. M3		
	ΔST ⩾ 2.32 ℃	ΔSAL ⩽ −0.24	ΔDen ⩽ −0.83 kg/m^3		ΔST > 3.5 ℃	SAL ⩽ −0.17	ΔDen ⩽ −1.04 kg/m^3
2, 3	√	×	√	1	√	×	√
5	×	×	×	8, 26	×	×	×
6, 29	√	×	√	9, 10, 17	√	√	√
7, 11, 12	√	√	√	18, 19, 20	√	√	√
13	√	×	×	21, 23, 24,	√	√	√
14, 15	√	√	√	25, 27, 28	√	√	√
16, 22	√	√	√	29	√	×	×

Note: √ indicates that the stratification factor thresholds are satisfied. × indicates that the stratification factor thresholds are not satisfied.

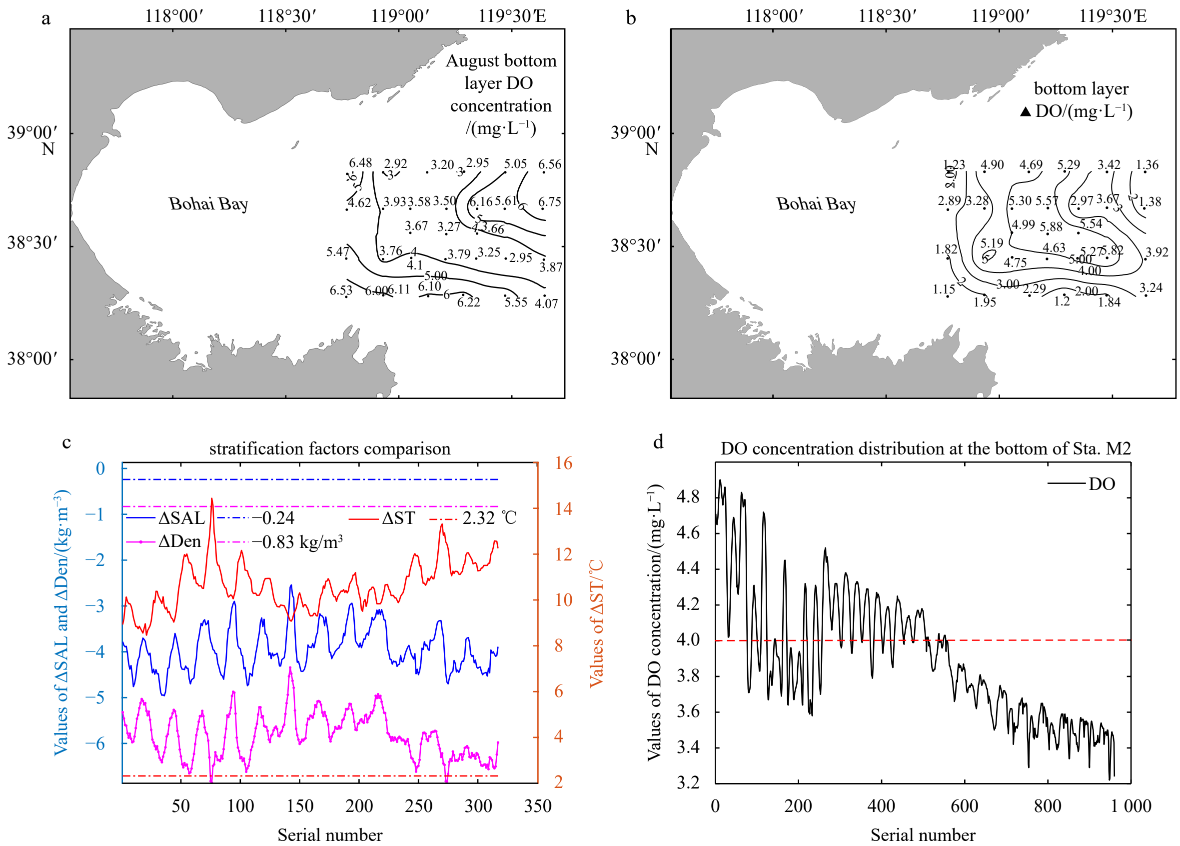

Fig. 6. Hypoxic validation of the August 2022 and 2023 data in the CBS. a. DO concentration distribution in the bottom layers at the 29 stations in August 2022 (black numbers: DO concentration values); b. distribution of bottom DO concentration values in June 2022 minus bottom DO concentration values (▲DO) in August at the 29 stations (black numbers:▲DO concentration values); c. comparison of ▲stratification factors (surface value minus bottom value) and SFTs (dotted line) in June 2023; and d. DO concentration distribution (the dash line is DO concentration = 4 mg/L) at the bottom at Sta. M2 during August 1–20, 2023.

cient between the SAL and DO concentration was only 0.45, the RMSE was 2.06 mg/L, and the R-squared value was 0.20, which were caused by the flow and sediment regulation of the nearshore rivers, especially the Huanghe River. However, the correlation coefficients of the ΔDO and the ΔST, ΔSAL, and ΔDen were close to $R \geqslant 0.78$, RMSE $\leqslant 1.05$, and R-squared $\geqslant 0.61$. Therefore, it is reasonable to evaluate the occurrence of hypoxic events using the differences in the stratification factors (ΔST, ΔSAL, and ΔDen) between the surface layer and the bottom layer.

In addition, consistent with the historical classification of the water health status in the BS, the data analysis, and published results, the stratification factors (ΔST, ΔSAL, and ΔDen) were found to be the principal factors assessing hypoxia in the CBS, and the hypoxic environment was defined as DO concentration < 4 mg/L, which is in line with the characteristics of the BS. As the spawning and breeding periods of economically important fish, shrimp, and crab in the BS are between March and August. The water dynamics are weak in summer, and the increases in the sea temperature and stratification prevent exchange between the water in the upper and lower layers. Frequent hypoxic events in the CBS threaten fishery resources in the Yellow and Bohai seas.

4.2 *Analysis of the factors affecting the evaluation of hypoxia in the CBS in 2022*

According to the evaluation and verification of the hypoxia in Section 3.5, hypoxia will occur at 19 stations in the study area. As a result, hypoxia occurred at 14 stations, of which 12 from 19 stations. Stations 6 and 8 were hypoxic stations in August, but they were not in evaluation stations. In particular, the ΔST, ΔSAL, and ΔDen at Sta. 8 did not meet the SFTs in June. However, in August, Sta. 8 was the hypoxic station with the lowest DO concentration value in the study area. As can be seen from Figs 7a and c, the surface layer at Sta. 8 received low ST and high SAL water from the north during the survey in early June, which interfered with the prediction. For the survey conducted at the end of August, it can be seen from Figs 7f and h that low ST and high SAL water entered the bottom layer near Stas 8, 9, and 18 from the north, resulting in enhanced stratification, which led to hypoxia at Sta. 8. As the water depth at Sta. 8 was the greatest among the stations with hypoxia, the DO concentration value of its bottom layer was the smallest during August. Due to the time lag of the formation of stratification at Sta. 8, the June forecast failed. As can be seen from Figs 7a–d, Sta. 6 was greatly affected by nearshore influences. In particular the SAL was influenced by the nearshore rivers, resulting in an excessive ΔSAL value in June, which could not be accurately evaluated.

A summer survey was conducted from August 30 to Septem-

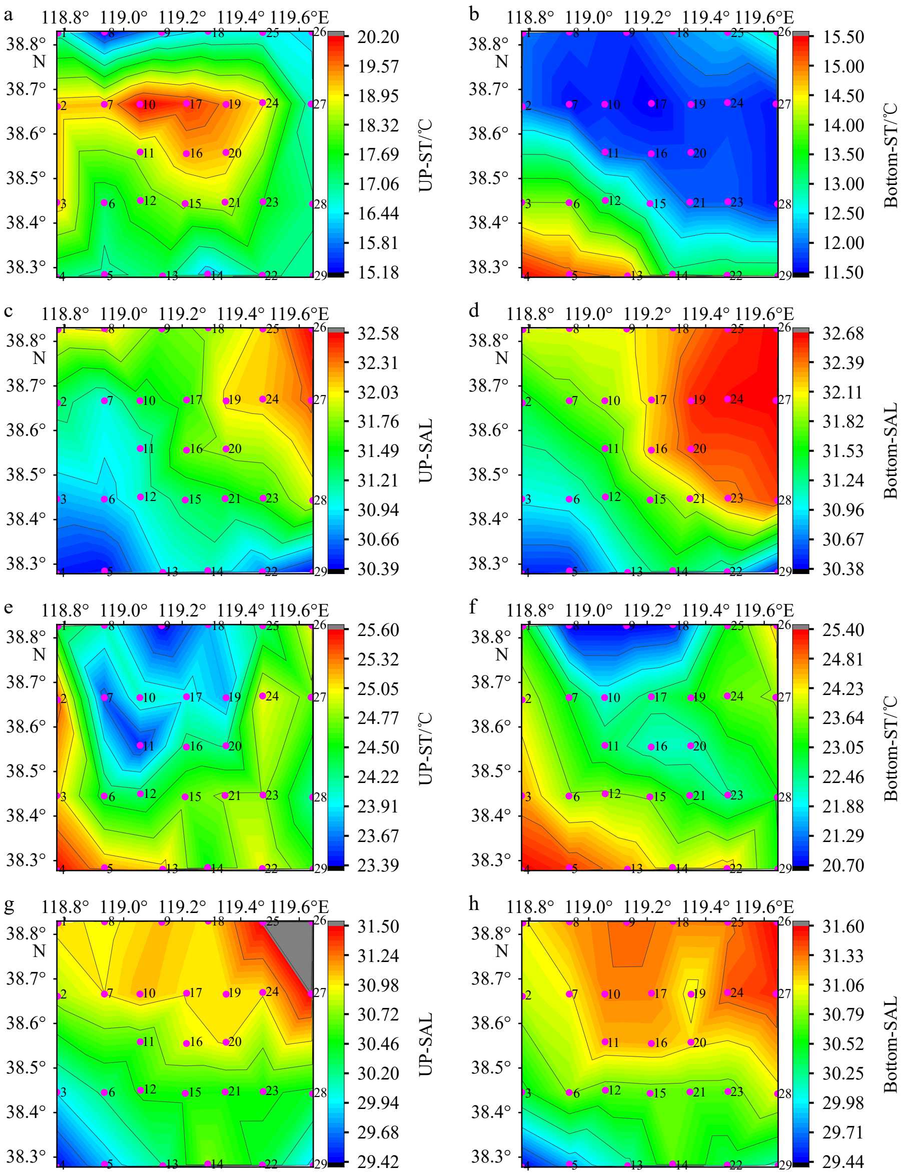

Fig. 7. ST and SAL distributions in June and August in 2022: a. up-ST in June; b. bottom-ST in June; c. up-SAL in June; d. bottom-SAL in June; e. up-ST in August; f. bottom-ST in August; g. up-SAL in August; and h. bottom-SAL in August. The pink dots and numbers represent the stations.

ber 4, 2022, in the CBS. However, between August 31 and September 2, gale force winds of 6 (Beaufort scale) and above occurred, and the ship was sheltered in the port. In Fig. 1b, the black station numbers indicate the period before the strong winds, and the red station numbers indicate the period after the strong winds during the summer of 2022. Stations 14, 24, 25, and 27 were investigated after the occurrence of strong winds. Although they were the stations that were about to experience hypoxia in the assessment in June, the survey data for August revealed that the DO concentration values were >4 mg/L and hypoxia did not occur, which should have been caused by the strong winds stirring the water and causing the DO concentration to rise. As can be seen from Fig. 7, the southwestern part of the study area was greatly affected by the nearshore area, the northeastern part was affected by the central bank of the BS, the western part was affected by Bohai Bay, the southern part was affected by Laizhou Bay, and the northwestern part was affected by the entry of low ST and high SAL water. In accordance with these observations, it was estimated in June that hypoxia was about to occur at Stas 12, 19, and 22; however, the data from August indicated that hypoxia did not occur at these stations.

5 Conclusions

In this study, we analyzed historical data for Stas M1, M2, and M3 in the CBS. The stratification of the CBS started in April, and it initially formed in June, which can be used to evaluate the occurrence of future hypoxic events. The stratification was strongest in August, which is the best time to observe the occurrence of hypoxia. It was found that it is feasible to predict the occurrence of hypoxia in August using the ΔST, ΔSAL, and ΔDen thresholds from June with the RAM analysis method. Thus the hypoxia SFTs in June were determined from the data Stas M1, M2, and M3, and the possibility of hypoxia occurring in the CBS in August 2022 and August 2023 was evaluated and verified using the measured data. It was found that stratification played a leading role in the occurrence of hypoxic events in the CBS. The stratification in the CBS was related to the seabed topography. The inflow of coastal rivers into the sea, windy days when hypoxia occurred, Bohai Bay, Laizhou Bay, the central bank of the BS, and the inflow of low temperature and high salinity water affected the stratification factors in the study area and interfered with the accuracy of the assessment.

Based on the analysis and assessment using data from 29 stations in the CBS at the end of May to early June in 2022, hypoxia will occur at 19 stations. The verification of the survey data from 29 stations at the end of August revealed the occurrence of hypoxia at 14 stations, of which 12 were evaluation stations, and the overall accuracy was 63%. Severe oxygen depletion occurred in the deep water area during August in 2022 in the CBS, the hypoxic values varied from 2.92 mg/L to 3.93 mg/L, and the depths of the hypoxic stations were greater than 22 m. The observation data for the area around Sta. M2 collected by a BTOMS in June 2023 were used to evaluate the possibility of hypoxia occurring in August based on the SFTs in June, and the observation data for August of the same year were used to verify that hypoxic events occurred in this region.

This method can only be used to evaluate hypoxic events with DO concentration values of <4 mg/L and cannot be used to characterize the severity of the hypoxia. Biological mineralization and degradation can promote the development of hypoxia. In the future, perhaps consideration of stratification, biodegradation, and mineralization can be used solve the severity of hypoxia.

Acknowledegements

This work was supported by the Data Center of Yantai Institute of Coastal Zone Research, Chinese Academy of Sciences, China. Some of the data and samples were collected utilizing R/V *Lanhai101* during open research cruise NORC2023-01, supported by the NSFC Shiptime Sharing Project under contrac No. 42249901.

References

Bao Xianwen, Wan Xiuquan, Wu Dexing, et al. 2004. Hydrologic characteristics of the end summertime in 2000 and early wintertime in the Bohai Sea. Haiyang Xuebao (in Chinese), 26(1): 14–24

Bulletin of the State of the Marine Environment of China, 2010. http://cn.chinagate.cn/reports/ 2011-06/08/content_22736793.htm

Chen Chung-Chi, Gong Gwo-Ching, Shiah Fuh-Kwo. 2007. Hypoxia in the East China Sea: one of the largest coastal low-oxygen areas in the world. Marine Environmental Research, 64(4): 399–408, doi: 10.1016/j.marenvres.2007.01.007

Conley D J, Humborg C, Rahm L, et al. 2002. Hypoxia in the Baltic Sea and basin-scale changes in phosphorus biogeochemistry. Environmental Science & Technology, 36(24): 5315–5320, doi: 10.1021/es025763w

Diaz R J. 2001. Overview of hypoxia around the World. Journal of Environmental Quality, 30(2): 275–281, doi: 10.2134/jeq2001.302275x

Ding Yang, Bao Xianwen, Yao Zhigang, et al. 2019. Observational and model studies of synoptic current fluctuations in the Bohai Strait on the Chinese continental shelf. Ocean Dynamics, 69(3): 323–351, doi: 10.1007/s10236-019-01247-5

Hagy J D, Boynton W R, Keefe C W, et al. 2004. Hypoxia in Chesapeake Bay, 1950–2001: long-term change in relation to nutrient loading and river flow. Estuaries, 27(4): 634–658, doi: 10.1007/BF02907650

Hetland R D, Dimarco S F. 2008. How does the character of oxygen demand control the structure of hypoxia on the Texas-Louisiana continental shelf? Journal of Marine Systems, 70(1/2): 49–62

Huang D J, Su J L, Backhaus J O. 1999. Modelling the seasonal thermal stratification and baroclinic circulation in the Bohai Sea. Continental Shelf Research, 19(11): 1485–1505, doi: 10.1016/S0278-4343(99)00026-6

Jiang Tao, Xu Yong, Liu Chuanxia, et al. 2016. Report on the occurrence of hypoxia in the central Bohai Sea. Progress in Fishery Sciences (in Chinese), 37(4): 1–6

Li Zhicheng, Wei Hao, Zhang Haiyan, et al. 2021. The interannual difference in summer bottom oxygen deficiency in Bohai Sea. Oceanologia et Limnologia Sinica (in Chinese), 52(3): 601–613

Li Daoji, Zhang Jing, Huang Daji, et al. 2002. Oxygen depletion off the Changjiang (Yangtze River) Estuary. Science in China Series D: Earth Sciences, 45(12): 1137–1146, doi: 10.1360/02yd9110

Lin Jing, Xie Lian, Pietrafesa L J, et al. 2006. Dissolved oxygen stratification in two micro-tidal partially-mixed estuaries. Estuarine, Coastal and Shelf Science, 70(3): 423–437

Lin Jing, Xu Hongzhou, Cudaback C, et al. 2008. Inter-annual variability of hypoxic conditions in a shallow estuary. Journal of Marine Systems, 73(1/2): 169–184, doi: 10.1016/j.jmarsys.2007.10.011

Locarnini R A, Mishonov A V, Baranova O K, et al. 2018. World Ocean Atlas 2018, Volume 1: Temperature (Technical report). NOAA Atlas NESDIS 81, https://www.researchgate.net/publication/335057554_World_Ocean_Atlas_2018_Volume_1_Temperature

Luo Lin, Li Shiyu, Li Hongmei. 2005. Characteristics of dissolved oxygen and its affecting factors in the Pearl River estuary in summer. Acta Scientiarum Naturalium Universitatis Sunyatseni (in Chinese), 44(6): 118–122

Rabalais N N, Díaz RJ, Levin L A, et al. 2010. Dynamics and distribution of natural and human-caused hypoxia. Biogeosciences, 7(2): 585–619, doi: 10.5194/bg-7-585-2010

Rabalais N N, Turner R E, Sen Gupta B K, et al. 2007. Hypoxia in the northern Gulf of Mexico: Does the science support the plan to reduce, mitigate, and control hypoxia? Estuaries and Coasts, 30(5): 753–772.

Rabalais N N, Turner R E, Wiseman Jr W J. 2002. Gulf of Mexico Hypoxia, A. K. A. “The Dead Zone”. Annual Review of Ecology, Evolution, and Systematics, 33: 235–263

Taft J L, Taylor W R. , Hartwig E O. et al. 1980. Seasonal oxygen depletion in Chesapeake Bay. Estuaries 3: 242–247. https://doi.org/10.2307/1352079

Turner R E, Schroeder W W, Wiseman W J. 1987. The role of stratification in the deoxygenation of Mobile Bay and adjacent shelf bottom waters. Estuaries, 10(1): 13–19, doi: 10.2307/1352020

Vaquer-Sunyer R, Duarte C M. 2008. Thresholds of hypoxia for marine biodiversity. Proceedings of the National Academy of Sciences of the United States of America, 105(40): 15452–15457

Wang Jinhua, Shen Yongming, Guo Yakun. 2010. Seasonal circulation and influence factors of the Bohai Sea: a numerical study based on Lagrangian particle tracking method. Ocean dynamics, 60(6): 1581–1596, doi: 10.1007/s10236-010-0346-7

Wei Hao, He Yunchang, Li Qingji, et al. 2007. Summer hypoxia adjacent to the Changjiang Estuary. Journal of Marine Systems, 67(3-4): 292–303, doi: 10.1016/j.jmarsys.2006.04.014

Wei Qinsheng, Wang Baodong, Yao Qingzhen, et al. 2019. Spatiotemporal variations in the summer hypoxia in the Bohai Sea (China) and controlling mechanisms. Marine Pollution Bulletin, 138: 125–134, doi: 10.1016/j.marpolbul.2018.11.041

Wei Hao, Zhao Liang, Zhang Haiyan, et al. 2021. Summer hypoxia in Bohai Sea caused by changes in phytoplankton community. Anthropocene Coasts, 4(1): 77–86, doi: 10.1139/anc-2020-0017

Wu R S S. 2002. Hypoxia: from molecular responses to ecosystem responses. Marine Pollution Bulletin, 45(1–12): 35–45, doi: 10.1016/S0025-326X(02)00061-9

Wu Xiao, Wu Hui, Wang Houjie, et al. 2019. Novel, repeated surveys reveal new insights on sediment flux through a narrow strait, Bohai, China. Journal of Geophysical Research: Oceans, 124(10): 6927–6941, doi: 10.1029/2019JC015293

Zhai Weidong, Zhao Huade, Zheng Nan, et al. 2012. Oxygen consumption and acidification of the bottom layer in the northwestern and northern coastal waters of the Bohai Sea in summer 2011. Chinese Science Bulletin (in Chinese), 57(9): 753–758, doi: 10.1360/csb2012-57-9-753

Zhang J, Gilbert D, Gooday A J, et al. 2010. Natural and human-induced hypoxia and consequences for coastal areas: synthesis and future development. Biogeosciences, 7(5): 1443–1467, doi: 10.5194/bg-7-1443-2010

Zhang Hua, Li Yanfang, Tang Cheng, et al. 2016. Spatial characteristics and formation mechanisms of bottom hypoxia zone in the Bohai Sea during summer. Chinese Science Bulletin, 61(14): 1612–1620, doi: 10.1360/N972015-00915

Zhang Yingying, Zhang Jing, Wu Ying, et al. 2007. Characteristics of dissolved oxygen and its affecting factors in the Yangtze Estuary. Environmental Science (in Chinese), 28(8): 1649–1654

Zheng Xiangyang, Zhang Hua, Li Yanfang, et al. 2021. The features and mechanisms of the North Shandong Coastal Current: a case study in 2014. Journal of Oceanography, 77(4): 631–646, doi: 10.1007/s10872-021-00597-3

Zhou Feng, Huang Daji, Xue Huijie, et al. 2017. Circulations associated with cold pools in the Bohai Sea on the Chinese continental shelf. Continental Shelf Research, 137: 25–38, doi: 10.1016/j.csr.2017.02.005

Zu Tingting, Bao Xianwen, Xie Jun, et al. 2005. Distribution and variation trends of the environmental factors in the central section of the Bohai Sea. Periodical of Ocean University of China (in Chinese), 35(6): 889–894